Photochemical Oxidation of Pt(IV)Me_3(1,2-Diimine) Thiolates to Luminescent Pt(IV)Sulphinates

*Barbora Mala,[a‡] Laura E. Murtagh,[a‡] Charlotte M. A. Farrow,[a] Geoffrey R. Akien,[a] Nathan R. Halcovich,[a] Sarah L. Allinson,[b] James A. Platts[c] and Michael P. Coogan[*a]*

a) Department of Chemistry, University of Lancaster, Lancaster, LA1 4YB, UK

b) Department of Biomedical and Life Sciences, University of Lancaster, Lancaster, LA1 4YG, UK

c) School of Chemistry, Cardiff University, Park Place, Cardiff, CF10 3AT, UK

ABSTRACT We report the formation of dinuclear complexes from, and photochemical oxidation of $(CH_3)_3$-Pt(IV)(N^N) (N^N = 1,2-diimine derivatives) complexes of thiophenolate ligands to the analogous sulphinates $(CH_3)_3Pt(N^N)(SO_2Ph)$ and structural, spectroscopic and theoretical studies of the latter revealing tuneable photophysics depending upon the 1,2-diimine ligands. Electron-rich thiolate and conjugated 1,2-diimines encourage formation of thiolate-bridged dinuclear complexes; smaller 1,2-diimines or electron poor thiolates favour mononuclear complexes. Photooxidation of the thiolate ligand yields hitherto unreported Pt(IV)-SO_2R complexes, promoted by electron deficient thiolates such as 4-nitrothiophenol, which exclusively forms the suphinate complex. Such complexes exhibit expected absorptions due to π - π* ligand transitions of the 1,2-diimines mixed with spin allowed singlet MLCT (d-π*) at relatively high energy (270 to 290 nm),

as well as unexpected broad, lower energy absorptions between 360 and 490 nm. DFT data indicate that these low energy absorption bands result from excitation of Pt-S and Pt-C σ- bonding electrons to π* orbitals on sulphinate and 1,2-diimine, the latter of which give rise to emission in the visible range.

Introduction

There are many applications of photophysically active transition-metal complexes in, amongst other areas, photocatalysis,[1] LEDs and related devices,[2] energy-related research and photovoltaics,[3] and luminescent cell imaging.[4] There are many well-known luminescent platinum-based systems, most involving d^8 Pt(II) complexes in particular tridentate cyclometallates derived from aromatic heterocycles with high quantum yields[5] and impressive 2-photon cross sections.[6] Certain platinum(IV) complexes also have useful photophysical properties including photoluminescence, with some showing quantum yields up to 80%.[7] Luminescent bis-cyclometalated Pt(IV) complexes, of the general formula $[Pt(C\hat{}N)_2(R)Cl]$, were first reported in 1984 by Chassot *et al*.,[8] and since then more brightly luminescent platinum (IV) complexes with high quantum yields and long luminescence lifetimes have been reported.[7] Cyclometalated Pt (IV) complexes are of particular interest as their properties, such as solubility and lipophilicity, are easily tuneable by only slight alterations of the ligands.[9] Furthermore, some luminescent tris-cyclometalated Pt (IV) complexes have displayed promising intense emission which is also highly sensitive to quenching by oxygen, making these potentially useful for oxygen sensing applications.[10] $Pt(IV)Me_3I$, the first transition-metal σ-alkyl complex ever reported,[11] is commercially available and exists as an iodide-bridged tetramer, and readily reacts with chelating N^N ligands to give mononuclear complexes of the general formula $PtMe_3(N\hat{}N)X$, analogous to the well-known luminophores $Re(CO)_3(N\hat{}N)(X)$ (X=Cl/Br) which have been widely applied in

sensing and imaging. The photochemistry and photophysics of the Pt(IV)(N^N) core have been widely studied[12] and there are several reports of thiolato-derivatives of this unit.[13]

There is one report exploring the synthesis, photophysics, and application in fluorescent cell imaging, of platinum (IV) 1,2-diimine trimethyl thiolates.[14] Time-dependent density functional theory calculations revealed that the excited states of platinum (IV) trimethyl 1,2-diimine iodide complexes arises from a mixed n and σ-π* Inter-Ligand Charge Transfer (ILCT) from the lone pair of sulphur and the S-Pt σ-bond, to the 1,2-diimine π*.[14] The small range of 1,2-diimines reported indicated that absorption and emission were tuneable by variations in ligand substitution, with emission extending into the NIR in one case. Therefore, in an effort to develop analogues with a variety of useful photophysical properties an investigation of complexes based on this general structure with a range of 1,2-diimine and thiolate ligands was undertaken.

Experimental

General Experimental

The starting materials, reagents and solvents used are all commercially available. ^{1}H-NMR and ^{13}C-NMR spectra were recorded at 400 and 100 MHz respectively on a Bruker Avance III 400 and referenced to residual solvent peaks. Chemical shifts are reported in ppm, and coupling constants in Hz. All photophysical measurements were recorded in acetonitrile at 20 C. UV vis spectra were recorded on an Agilent Technologies Cary 60. IR spectra were recorded on an Agilent Technologies Cary 630 FTIR Spectrometer as solids and are reported in wavenumbers (cm^{-1}). Mass spectra were recorded on Shimadzu LCMS-IT-TOF in ESI+ mode.

Steady state emission and excitation spectra were recorded on an Agilent Technologies Cary Eclipse. Luminescence lifetimes were recorded on a PicoQuant FluoTime 300 exciting with an LDH-P-C-375 or LDH-P-C405 picosecond pulsed laser (PicoQuant) operating at 50MHz and

80MHz respectively. The emission signals were digitised using a high-resolution TCSPC module (PicoHarp 300, PicoQuant) with 25 ps time width per channel. The time resolved decay curves were analysed using FLUOFIT software (PicoQuant) using a one-exponential model. Quantum yields were estimated relative to $[Ru(bpy)_3].2PF_6$ in aerated acetonitrile with titration to equi-absorbing solutions at the excitation wavelengths at around A = 0.05. Degassed measurements were recorded in a quartz cuvette fused to a T-piece connecting a round bottom flask and J Young tap connecting a ground glass joint, following 3 cycles of freeze-pump-thaw degassing. Iodotrimethyl(N^N)Pt(IV) complexes **1-5** (N^N = 2,2'-bipyridine (bpy) **1**, 4,4'-dimethoxy-2,2'-bipyridine (OMebpy) **2**, 1,10-phenanthroline (phen) **3**, 4,7-diphenyl-1,10-phenanthroline (Bphen) **4**, dipyrido[3,2-a:2',3'-c]phenazine (DPPZ) **5**) were prepared by literature procedures.[12,14] Complexes **6-25** derived from the reactions of **1-5** with thiophenol, and derivatives were metastable and for details relating to their detection, partial characterisation by crystallography and in some cases NMR, for details of the mechanistic studies and for preparation of authentic sample of 4-mercaptomethylbenzoate disulphide[15] see SI.

$[PtMe_3(bpy)SO_2PhNO_2]$ 26.

To a flask containing $[PtMe_3I(2,2'\text{-bipyridine})]$ **1** (101.3 mg, 0.19 mmol), 4-nitrothiophenol (30.0 mg, 0.19 mmol) and NaO^tBu (20.6 mg, 0.21 mmol) was added acetonitrile (4 mL) and water (1 mL) and the mixture heated at 60 °C for 30 minutes then cooled to room temperature and refrigerated overnight giving a solution containing orange crystals and white powder. The mixture was filtered and washed with water to obtain orange crystals **26** (63.1 mg, 57%).

δ ^{1}H NMR (400 MHz, CD_3CN): 8.79 (2H, d, J = 6.5 Hz, H6/6'; ^{195}Pt satellite J = 19.5 Hz), 8.19 (2H, d, J = 8.2 Hz, H3/3'), 8.07 (2H, t, J = 7.9 Hz, H4/4'), 7.67 (2H, t, J = 6.6, H5/5'), 7.34 (2H, d, J = 8.9 Hz, H8/8'), 6.58 (2H, d, J = 9.1 Hz, H7/7'), 1.17 (6H, s, eq-Me; ^{195}Pt satellite J = 70.2

Hz), 0.32 (3H, s, ax-Me; ^{195}Pt satellite J = 66.2 Hz); ^{13}C NMR 158.8, 154.1, 146.6 (^{195}Pt satellite J = 14.3 Hz) 139.0, 134.2 (^{195}Pt satellite J = 6.3 Hz), 127.1 (^{195}Pt satellite J = 14.4 Hz), 123.9 (^{195}Pt satellite J = 8.5 Hz), 121.5, -0.8 (^{195}Pt satellites obscured by solvent signal), -6.4 (^{195}Pt satellite J = 677.1 Hz); IR υ_{max} (cm^{-1}) 2892, 2812, 1559, 1491, 1418, 1219; Crystal Data for **26** $C_{19}H_{21}N_3O_4PtS$ (M =582.54 g/mol): triclinic, space group P-1 (no. 2), a = 6.96733(19) Å, b = 8.8748(2) Å, c = 15.4326(4) Å, α = 93.374(2)°, β = 92.851(2)°, γ = 92.314(2)°, V = 950.52(4) Å^3, Z = 2, T = 100.00(10) K, μ(Mo Kα) = 7.523 mm^{-1}, *Dcalc* = 2.035 g/cm^3, 21289 reflections measured (6.802° ≤ 2Θ ≤ 59.066°), 4782 unique (R_{int} = 0.0372, R_{sigma} = 0.0267) which were used in all calculations. The final R_1 was 0.0181 (I > 2σ(I)) and wR_2 was 0.0410 (all data). CCDC 2013232.

[PtMe$_3$(1,10-phenanthroline)SO$_2$PhNO$_2$] 27.

To a flask containing [PtMe$_3$I(1,10-phenanthroline)] **3** (24.9 mg, 0.05 mmol), 4-nitrothiophenol (7.40 mg, 0.05 mmol) and NaO^{t}Bu (5.2 mg, 0.05 mmol) was added acetonitrile (4 mL) and water (1 mL) and the mixture heated at 60 °C for 30 minutes then cooled to room temperature and refrigerated overnight giving a solution containing orange crystals and white powder. The mixture was filtered and washed with water to obtain orange crystals **27** (19.6 mg, 71%).

δ ^{1}H NMR (400 MHz, $CDCl_3$): 9.14 (2H, d, J = 5.0 Hz, H2/2'; ^{195}Pt satellite J = 19.1), 8.59 (2H, d, J = 8.3 Hz, H4/4'), 8.03 – 7.98 (4H, m, H5/5' and H3/3'), 6.92 (2H, d, J = 8.9 Hz H7/7'), 6.16 (2H, d, H6/6'), 1.33 (6H, s, eq-Me; ^{195}Pt satellite J = 70.9 Hz), 0.40 (3H, s, ax-Me; ^{195}Pt satellite J = 66.4 Hz); δ ^{13}C NMR (400 MHz, $CDCl_3$) 157.4, 146.5 (^{195}Pt satellite J = 15.2 Hz), 145.5, 142.8, 137.2, 133.7 (^{195}Pt satellite J = 5.2 Hz), 130.8 (^{195}Pt satellite J = 6.4 Hz), 127.4, 125.3 (^{195}Pt satellite J = 14.0 Hz), 120.8, -0.0, -5.7 (^{195}Pt satellite J = 681.8 Hz); IR υ_{max} (cm^{-1}) 2886, 2808, 1567, 1483, 1425, 1219; Crystal Data for **27** $C_{21}H_{21}N_3O_4PtS$ (M =606.56 g/mol): monoclinic, space group

$P2_1/n$ (no. 14), a = 6.87831(12) Å, b = 13.65275(18) Å, c = 21.0623(3) Å, β = 97.2931(15)°, V = 1961.91(5) Å^3, Z = 4, T = 99.99(10) K, μ(Cu Kα) = 14.681 mm^{-1}, *Dcalc* = 2.054 g/cm^3, 19671 reflections measured (7.736° ≤ 2Θ ≤ 152.948°), 4087 unique (R_{int} = 0.0423, R_{sigma} = 0.0255) which were used in all calculations. The final R_1 was 0.0365 (I > 2σ(I)) and wR_2 was 0.0967 (all data). CCDC 2013233.

[PtMe$_3$(4,7'-diphenyl-1,10-phenanthroline)SO$_2$PhNO$_2$] 28.

To a flask containing [PtMe$_3$I(4,7'-diphenyl-1,10-phenanthroline)] **4** (25.7 mg, 0.04 mmol), 4-nitrothiophenol (5.9 mg, 0.04 mmol) and NaO^{t}Bu (3.9 mg, 0.04 mmol) was added acetonitrile (4 mL) and water (1 mL) and the mixture heated at 60 °C for 30 minutes then cooled to room temperature and refrigerated overnight giving a solution containing orange crystals and white powder. The mixture was filtered and washed with water to obtain orange crystals **28** (10.3 mg, 38%).

δ ^{1}H NMR (400 MHz, $CDCl_3$): 9.18 (2H, d, J = 5.2 Hz, H2/2'; ^{195}Pt satellite J = 19.3), 7.91 (2H, s, H4/4'), 7.85 (2H, d, 5.2 Hz, H3/3'), 7.67 – 7.51 (10H, m, Ph), 7.11 (2H, 9.0 Hz, d, H9/9'), 6.44 (2H, 6.4 Hz, d, H8/8'), 1.45 (6H, s, eq-Me; ^{195}Pt satellite J = 70.0 Hz), 0.53 (3H, s, ax-Me; ^{195}Pt satellite J = 66.6 Hz); δ ^{13}C NMR (400 MHz, $CDCl_3$) 156.9, 150.5, 146.0, 145.8 (^{195}Pt satellite J = 14.7 Hz), 143.0, 135.6, 134.0, 129.8, 129.5, 129.2, 129.1, 125.6, 125.4, 120.8, 0.1, -5.4 (^{195}Pt satellite J = 678.0 Hz); IR υ_{max} (cm^{-1}) 2890, 2812, 1560, 1489, 1217; Crystal data for **28** $C_{33}H_{29}N_3O_4PtS$ (M =758.74 g/mol): monoclinic, space group C2/c (no. 15), a = 21.3317(3) Å, b = 12.75780(10) Å, c = 24.8460(3) Å, β = 110.718(2)°, V = 6324.47(15) Å^3, Z = 8, T = 100.0(3) K, μ(CuKα) = 9.245 mm^{-1}, *Dcalc* = 1.594 g/cm^3, 48486 reflections measured (7.608° ≤ 2Θ ≤ 152.926°), 6617 unique (R_{int} = 0.0305, R_{sigma} = 0.0135) which were used in all calculations. The final R_1 was 0.0437 (I > 2σ(I)) and wR_2 was 0.0987 (all data). CCDC 2013234.

[PtMe$_3$(dipyrido[3,2-a:2',3'-c]phenazine)SO$_2$PhNO$_2$] 29.

To a flask containing [PtMe$_3$I(dipyrido[3,2-a:2',3'-c]phenazine)] **5** (25.5 mg, 0.04 mmol), 4-nitrothiophenol (6.2 mg, 0.04 mmol) and NaO^{t}Bu (4.5 mg, 0.04 mmol) was added acetonitrile (4 mL) and water (1 mL) and the mixture heated at 60 °C for 30 minutes then cooled to room temperature and refrigerated overnight giving a solution containing orange crystals and white powder. The mixture was filtered and washed with water to obtain orange crystals **29** (20.1 mg, 76%).

δ ^{1}H NMR (400 MHz, $CDCl_3$): 9.80 (2H, d, J = 8.2 Hz, H4/4'), 9.18 (2H, d, J = 5.1 Hz, H2/2'; ^{195}Pt satellite J = 18.7), 8.50 – 8.44 (2H, m, H5/5'), 8.10 – 8.05 (4H, m, H6/6' and H3/3'), 7.02 (2H, d, J = 8.9, H8/8'), 6.48 (2H, d, J = 8.9, H7/7'), 1.44 (6H, s, eq-Me; ^{195}Pt satellite J = 70.5 Hz), 0.53 (3H, s, ax-Me; ^{195}Pt satellite J = 64.6 Hz); **29** was insufficiently soluble to collect 13C data. IR υ_{max} (cm^{-1}) 2892, 2812, 1560, 1491, 1418, 1221; Crystal Data for **29** $C_{27}H_{23}N_5O_4PtS$ (*M* =708.65 g/mol): monoclinic, space group $P2_1/m$ (no. 11), *a* = 7.98930(10) Å, *b* = 13.0769(2) Å, *c* = 12.1911(2) Å, *β* = 97.1620(10)°, *V* = 1263.73(3) Å^3, *Z* = 2, *T* = 215.00(10) K, μ(Cu Kα) = 11.536 mm^{-1}, *Dcalc* = 1.862 g/cm^3, 13560 reflections measured (7.308° ≤ 2Θ ≤ 153.144°), 2755 unique (R_{int} = 0.0501, R_{sigma} = 0.0320) which were used in all calculations. The final R_1 was 0.0496 (I > 2σ(I)) and wR_2 was 0.1303 (all data). CCDC 2013235.

Computational Procedures.

DFT calculations used Gaussian09[16]: geometry optimisation of **26** was performed using M06-2X/6-31+G(d,p) with SDD ECP/basis on Pt[17] , which retains the stacking interaction between bipy and Ar-NO$_2$. Predicted absorption spectra and orbital plots were obtained from CAM-B3LYP[18] with the same basis set as optimisation, in PCM simulation of CH_3CN[19].

Crystal Structures were solved and refined using OLEX[20] running the SHELX[21] suite of programs and images generated in ORTEP.[22]

Results and Discussion

Reactions of Iodotrimethyl Platinum (IV) 1,2-Diimines with Thiophenolates.

Following the literature precedent[12,14] iodotrimethylplatinum (IV) 1,2-diimines were prepared from reaction of $[PtMe3I]_4$ with the relevant 1,2-diimine ligand (i.e. N^N = 2,2'-bipyridine (bpy) **1**, 4,4'-dimethoxy-2,2'-bipyridine (OMebpy) **2**, 1,10-phenanthroline (phen) **3**, 4,7-diphenyl-1,10-phenanthroline (Bphen) **4**, dipyrido[3,2-a:2',3'-c]phenazine (DPPZ) **5**) in toluene at reflux for in good to excellent yields (Scheme 1). The DPPZ derivative **5** had low solubility in all solvents, however, despite the small size of the crystals obtained, X-ray data of sufficient quality to establish connectivity were obtained confirming the identity of the product.

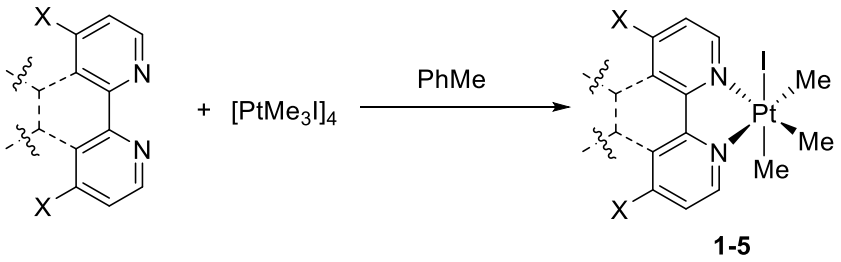

Scheme 1. Synthesis of iodotrimethylplatinum(IV) complexes **1-5 (1** = Bpy, **2** = di-OMebpy, **3** = phen, **4** = Bphen, **5** = DPPZ)

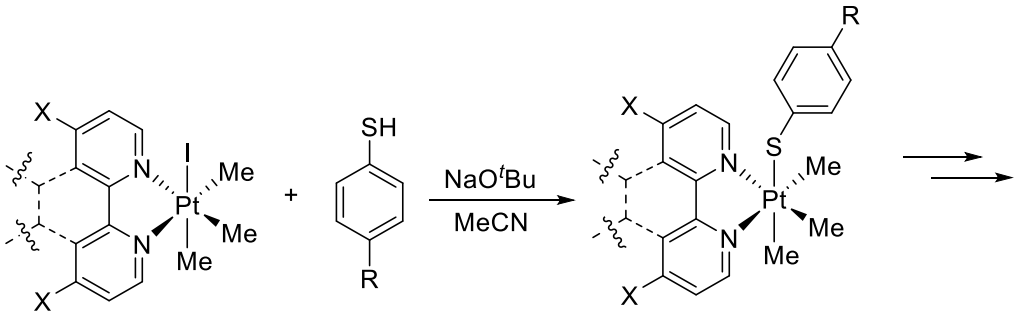

Scheme 2. General reaction of iodotrimethylpatinum (IV) 1,2-diimines with thiophenols R, X = H, CO_2Me, OMe, NO_2.

Attempts to prepare the thiolate complexes derived from iodoplatinum species **1-5** following literature precedent (Scheme 2),[14] however, led not to the expected products but to a series of metastable complexes which were not fully characterized, but the identity of some were established by NMR and X-ray crystallography. NMR (See SI) indicated that an equilibrium existed between mononuclear and dinuclear products in many cases, e.g. **6** and **7** from the reaction of **5** with 4-mercaptomethylbenzoate (Scheme **3**, Figure **1**), and examples of the dinuclear structures were also confirmed by X-ray crystallography.

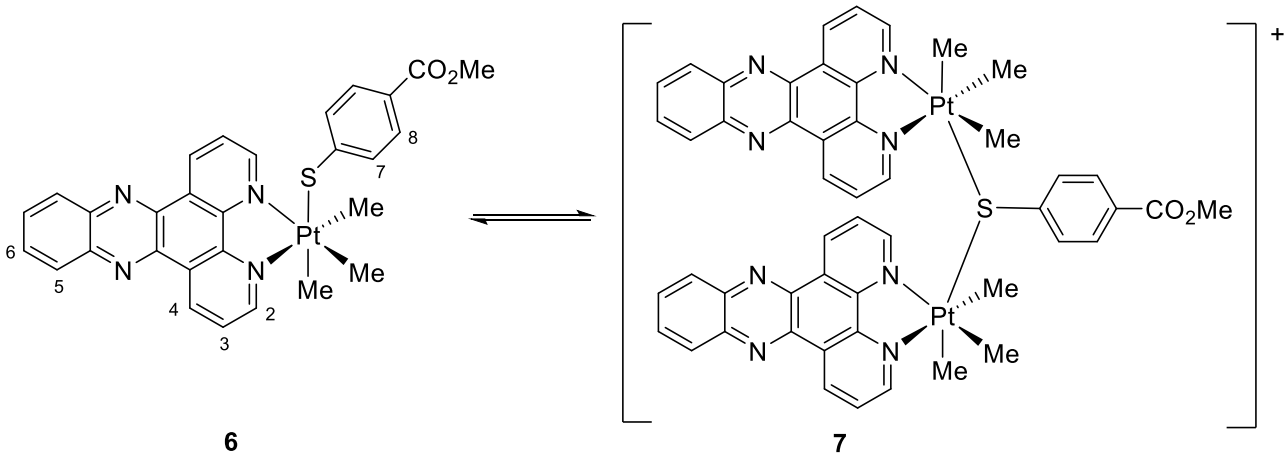

6 **7**

Scheme 3. 2 $PtMe_3dppzSC_6H_4$ -4-CO_2Me **6** ⇋ $[(PtMe_3dppz)_2SC_6H_4$-4-$CO_2Me]^+$ **7**

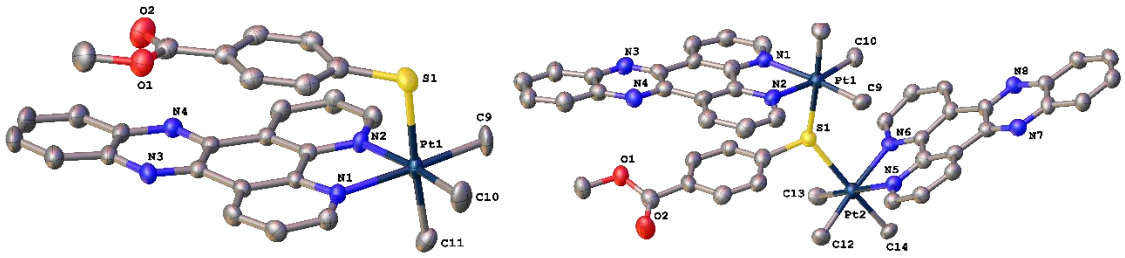

Figure 1. Thermal ellipsoid plots of $Me_3dppzPtSC_6H_4$-4-CO_2Me **6** (LHS) and the cationic fragment of $[(Me_3dppzPt)_2SC_6H_4$-4-$CO_2Me]PF_6$ **7** (RHS) (Hydrogen atoms omitted for clarity).

In other cases NMR analysis indicated the presence of only mononuclear species, and X-ray crystallography showed either the expected mononuclear thiophenolate complex, or a sulphinate complex in which the coordinated sulphur had acquired two oxygen atoms. Examples of these are given in Scheme 4 and Figure 2 (thiolate **11**) and Scheme 5 and Figure 3 (sulphinate **12**) the rest of the observed species are summarized in Table 1, and further details are available in SI. Again, attempts to purify and characterize these species, with the exception of those derived from 4-nitrothiophenol, led to decomposition to complex product mixtures.

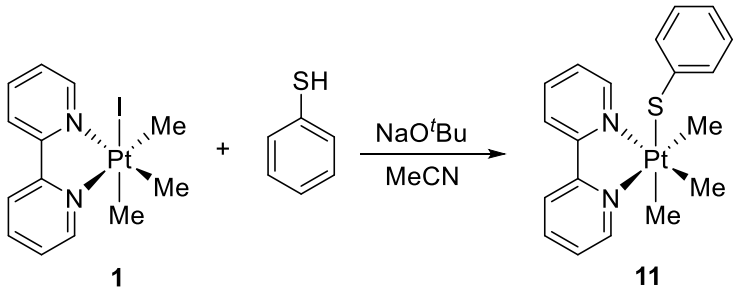

1 **11**

Scheme 4. Synthesis of $Me_3bpyPtSPh$ **11**

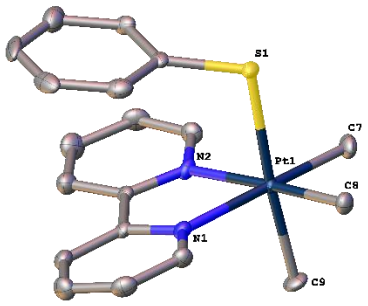

Figure 2. Thermal ellipsoid plot of $Me_3bpyPtSPh$ **11** (hydrogen atoms omitted for clarity).

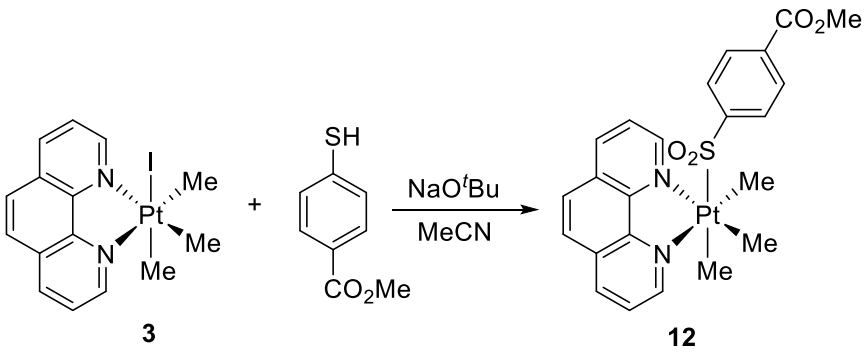

Scheme 5. Synthesis of $Me_3PhenPtSO_2$-4-C_6H_4-CO_2Me **12**

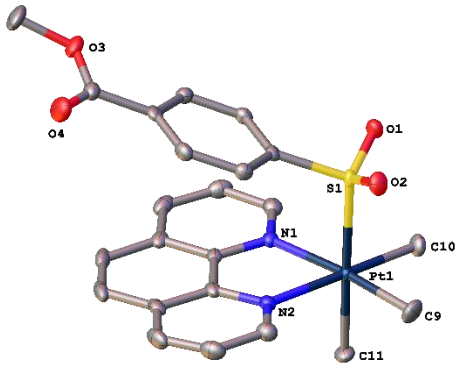

Figure 3. Thermal ellipsoid plot of $Me_3PhenPtSO_2$-4-C_6H_4-CO_2Me **12** (hydrogen atoms omitted for clarity).

Regardless of the unstable nature of the products, crystallographic characterization of these species was interesting as an addition to the previously known S-bridged multinuclear Pt(IV)Me_3 species,[23] and revealing the first examples of crystallographically characterised Pt(IV) sulphinate complexes.

Although many of these complexes are metastable and not fully characterised, the observations of cases in which dinuclear complexes (**7**, **9**, **14**, **16**) were apparent in the NMR spectra suggest that electron-rich thiolate and conjugated 1,2-diimines encourage formation of thiolate-bridged dinuclear complexes while the cases in which mononuclear species dominate (**11**, **13**, **15**, **21**, **30**) suggest that smaller 1,2-diimines or electron poor thiolates favour mononuclear complexes

N^N	4-R-Ar-SH, R=	Product Type	Number	Crystal Structure (counterion; origin)	NMR Data
DPPZ	CO_2Me	Mono⇋dinuclear	**6**	Mononuclear	Equilibrium 6-7
DPPZ	CO_2Me	Dinuclear	**7**	Dinuclear (PF_6;added)	
Bpy	OMe	Mononuclear	**8**		Equilibrium 8-9
Bpy	OMe	Dinuclear	**9**	Dinuclear complex(S_2O_7; from $MgSO_4$)	
Bpy	OMe	Dinuclear	**10**	Dinuclear complex(4-MeO-Ar-SO_3^-; oxidation)	
Phen	H	Mononuclear	**11**		Mononuclear
Phen	CO_2Me	Sulphinate	**12**		Mononuclear
Phen	H	Mono⇋dinuclear	**13**	Thiolate	Mono⇋dinuclear
Phen	OMe	Mono⇋dinuclear	**14**		Mono⇋dinuclear
BPhen	H	Mononuclear	**15**	Sulphinate	Mononuclear
BPhen	OMe	Mono⇋dinuclear	**16**		Mono⇋dinuclear
BPhen	CO_2Me	Mono⇋dinuclear	**17/18**	Thiolate	Mono⇋dinuclear
OMeBpy	H	Mono⇋dinuclear	**19**		Mono⇋dinuclear
OMeBpy	OMe	Mono⇋dinuclear	**20**		Mono⇋dinuclear
OMeBpy	CO_2Me	Mononuclear	**21**	Thiolate	Mononuclear
Bpy	NO_2	Sulphinate	**26**	Sulphinate	Sulphinate
Phen	NO_2	Sulphinate	**27**	Sulphinate	Sulphinate
BPhen	NO_2	Sulphinate	**28**	Sulphinate	Sulphinate
DPPZ	NO_2	Sulphinate	**29**	Sulphinate	Sulphinate
OMeBpy	NO_2	Mononuclear	**30**	Mononuclear	Mononuclear

Table 1. Indications of product nature from crystallographic and NMR data. See SI Scheme S2 for chemical structures of all substances.

Structural Studies of Thiolate and Sulphinate Complexes of the $PtMe_3$(N^N) Core.

X-Ray crystallography showed that all products form distorted octahedra whether in mononuclear or dinuclear form. Table 2 summarises the bond lengths of most interest. The Pt-S bonds are all of similar lengths, however, the Pt-S bonds in sulphinate complexes (**12**, **17, 26-29**) are shorter that those in the other complexes. A search of the Cambridge Crystallographic Data Centre for structures containing the Pt-SO_2R unit found only twenty three reports of this substructure, of these twenty were cyclic[24-27] (i.e. contained a chelating O_2S^D unit, D = donor atom), meaning that only three unsupported Pt-SO_2 bonds have previously been characterised, and there were no Pt(IV) sulphinates reported.

Even though the number of crystal structures containing Pt-SO_2R bonds is limited, a few of the reports highlight Pt-S bond shortening upon oxidation of sulphur.[25,26] This is unexpected as one would expect this bond to get longer as the sulphur becomes a weaker sigma donor. However, there are reported to be three factors that determine the M-S bond length, from analogy with Ni-S complexes. In these too, shortening of the Ni-S bond was also observed with increasing sulphur oxidation.[28] Although the sulphur becomes a poorer sigma donor as it is oxidised, the sulphur atom also contracts in size upon oxidation, and there is less electronic repulsion between the metal *d*-orbitals and sulphur due to loss of its lone pairs. Overall, the latter two effects dominate over the reduced sigma donation, thus resulting in a shorter Pt-S bond length.

The dinuclear complexes **7, 9** and **10** have slightly longer Pt-S bonds, as expected from the bridging nature of the formally monoanionic thiolate. Interestingly, the two Pt-S bonds in **7** and **9** are of different lengths, as are their respective Pt-C_{ax} bonds with, in each case, the segment with the shorter Pt-S bond showing a longer Pt-C_{ax} and vice versa, which is assigned to the *trans*-influence. Complex **17** ($PtMe_3BPhenSC_6H_4CO_2Me$) displays the longest Pt-S bond along with the

shortest Pt-C_{ax} bond, resulting from the electron withdrawing -CO_2Me group reducing both the donor strength and trans influence of the thiolate.

Complex	**N^N Ligand**	**S-Ligand**	**Pt-S (Å)**	**Pt-C_{ax}(Å)**
6	DPPZ	S-C_6H_4-CO_2Me	2.479	2.073
7i	DPPZ	S-C_6H_4-CO_2Me	2.567	2.043
7ii	(dinuclear, PF_6)		2.504	2.050
9i	bpy	S-C_6H_4-OMe	2.482	2.071
9ii	(dinuclear, $S_2O_4^{2-}$)		2.505	2.062
10	bpy	S-C_6H_4-OMe	2.493	2.064
10	(dinuclear, MeO- C_6H_4-SO_3^{2-})		2.483	2.069
11	bpy	S-Ph	2.460	2.079
12	phen	SO_2-C_6H_4-CO_2Me	2.391	2.074
15	bathophen	SO_2-Ph	2.392	2.092
17	bathophen	S-C_6H_4-CO_2Me	2.552	2.042
21	4,4'-diOMe-bpy	S-C_6H_4-CO_2Me	2.480	2.064
26	Bpy	SO_2-C_6H_4-NO_2	2.404	2.086
27	Phen	SO_2-C_6H_4-NO_2	2.434	2.083
28	BPhen	SO_2-C_6H_4-NO_2	2.411	2.064
29	DPPZ	SO_2-C_6H_4-NO_2	2.456	2.112
30	4,4'-diOMe-bpy	S-C_6H_4-NO_2	2.502	2.082

Table 2: Pt-S and Pt-C_{axial} bond lengths obtained from X-Ray crystallography.

Mechanistic Studies of Dinuclear Complex Formation and Oxidation.

In addition to the above observations of the formation of dinuclear complexesand sulphinates, further information regarding the degradation of these complexes came from the study of the degradation of $PtMe_3BpySC_6H_4CO_2Me$, **22. 22** had previously been reported to be stable[14] however, a solution of **22** in $CDCl_3$ which had been aged for 6 weeks yielded two different types of crystals which X-Ray diffraction revealed to be chlorotrimethyl-(2,2'-bipyridine) -platinum (IV), previously uncharacterised by crystallography, but closely related to the iodo-and bromo-analogues which have been,[29] and 4-mercaptomethylbenzoate disulphide.[15] The abstraction of chloride from chloroform and displacement of the thiolate hinted at a more complex chemistry than simple aerobic oxidation of coordinated thiols to sulphinates and an equilibrium of mononuclear and dinuclear species which had been observed above.

In order to further investigate the degradation of **22**, it was studied in CD_3CN in order to avoid halide exchange phenomena, deliberately exposing the sample to air over 72 hours and following the changes by ^1H NMR. NMR analysis revealed that at least three products were present which DOSY suggested had significantly different masses. Although molecular mass calculations from diffusion DOSY data are inaccurate for systems containing atoms heavier than sulphur, and the calculation has not been optimised for this solvent, the order of masses was clear from the diffusion coefficients, and comparison with the mononuclear complex **12** (previously characterised), and iodide **1** (previously characterised, no thiolate peaks) allowed the dinuclear complex(new species showing both bpy and thiolate peaks in a 2:1 ratio) and other heavier species to be identified in the mixture. (Figure 4, Scheme 6).

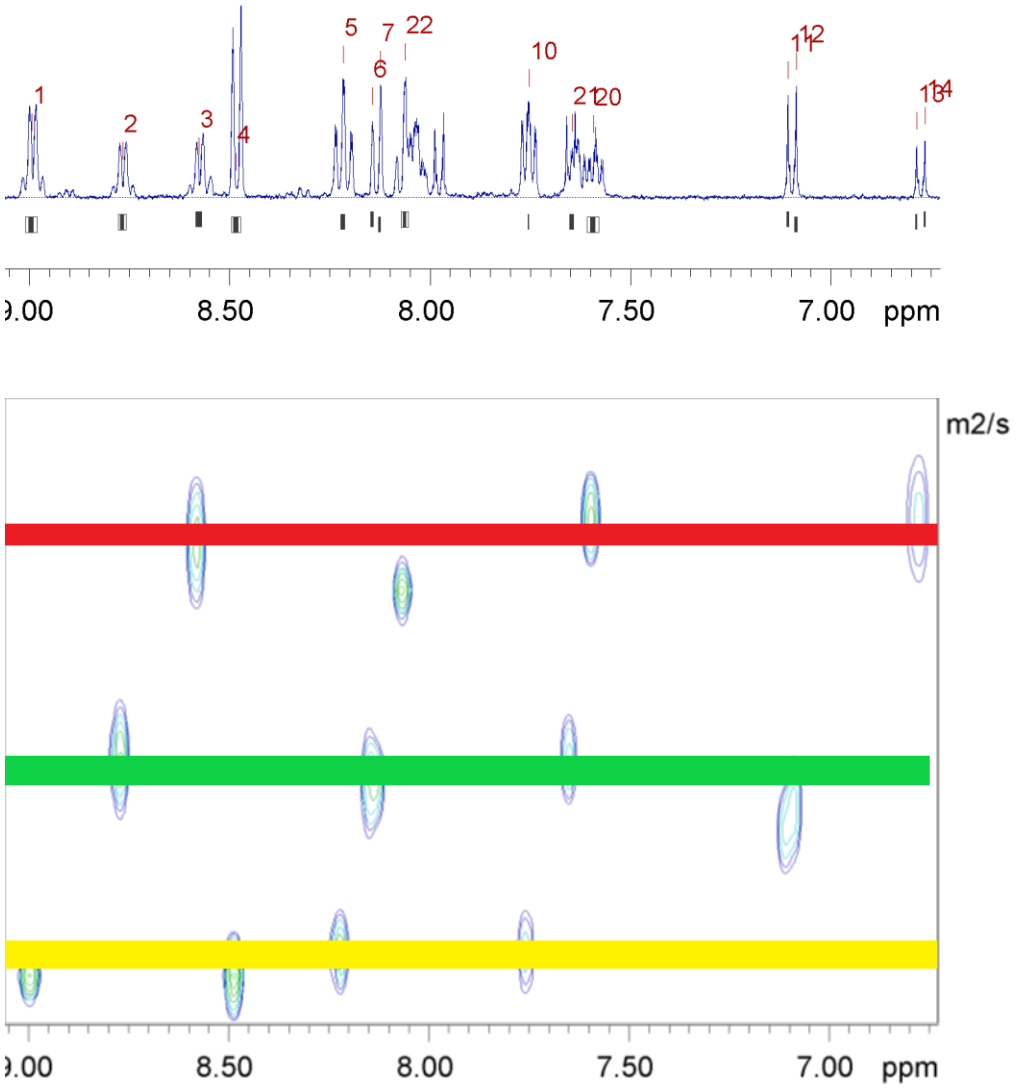

Figure 4: DOSY NMR showing the diffusion of dinuclear complex(red, D_{AV} = 1.40 x 10^{-9} m^2/s, mass = 959), mononuclear complex(green, D_{AV} = 1.66 x 10^{-9} m^2/s, mass = 563), and iodide **1** (yellow, D_{AV} = 1.86 x 10^{-9} m^2/s, mass = 523).

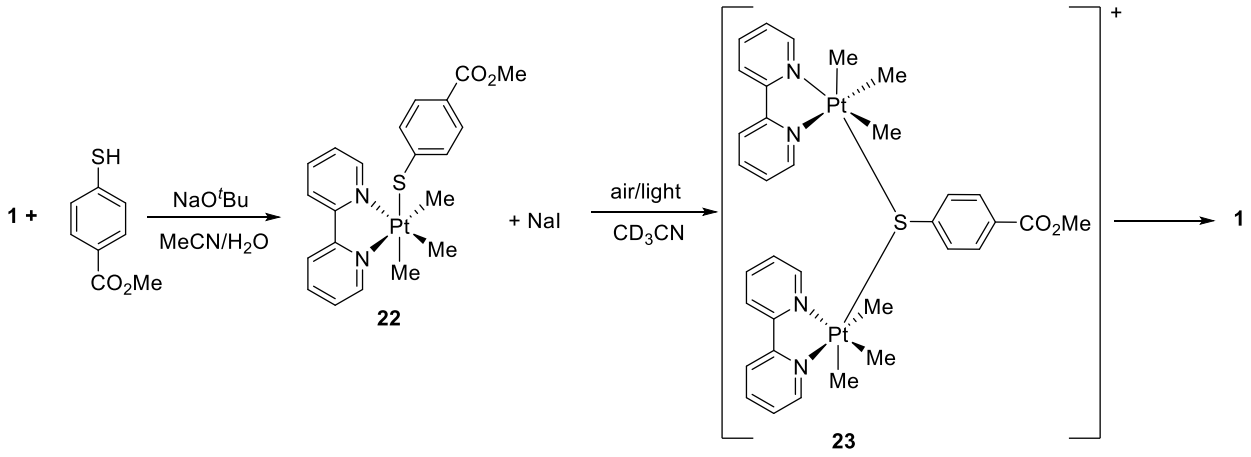

Scheme 6: Decomposition of 22.

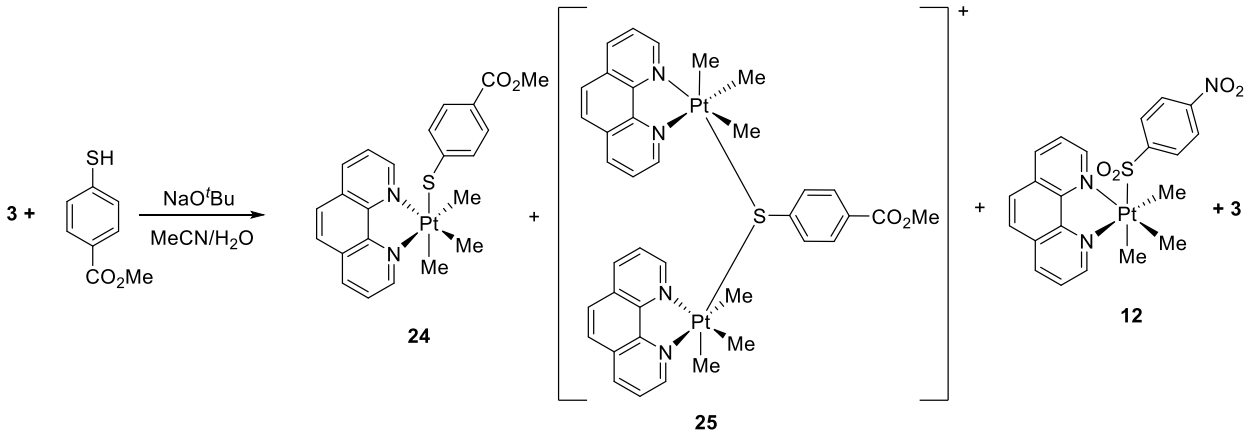

Scheme **7**. Preparation and photolytic degradation of $Me_3PhenPtS\text{-}4\text{-}C_6H_4\text{-}CO_2Me$ **24**.

A series of NMR experiments following the degradation of **22** (Scheme 6) and *in situ* prepared **24** (Scheme 7, Figure 5) under aerobic and anaerobic atmospheres, and in amber and clear tubes demonstrated that the conversion of mononuclear complexes to dinuclear complexesand / or sulphinates required both light and air, and revealed a solution species differing in exact chemical shift from, but of similar mass to, the mononuclear complexes, assigned as the sulphinates. Under anaerobic conditions the samples were stable even under irradiation (300 Lumen white LED light source, see SI for output profile), and, in the absence of light, aerobic samples were also stable.

Following the photo-degradation of **22** and **24** and by comparing signals to known materials, and DOSY estimations of mass, the identity of the species (thiolate, dinuclear complex, disulphide, sulphonic acid and sulphinate complex) and the sequence of generation was determined (see ESI for details of the reasoning behind identification of peaks).

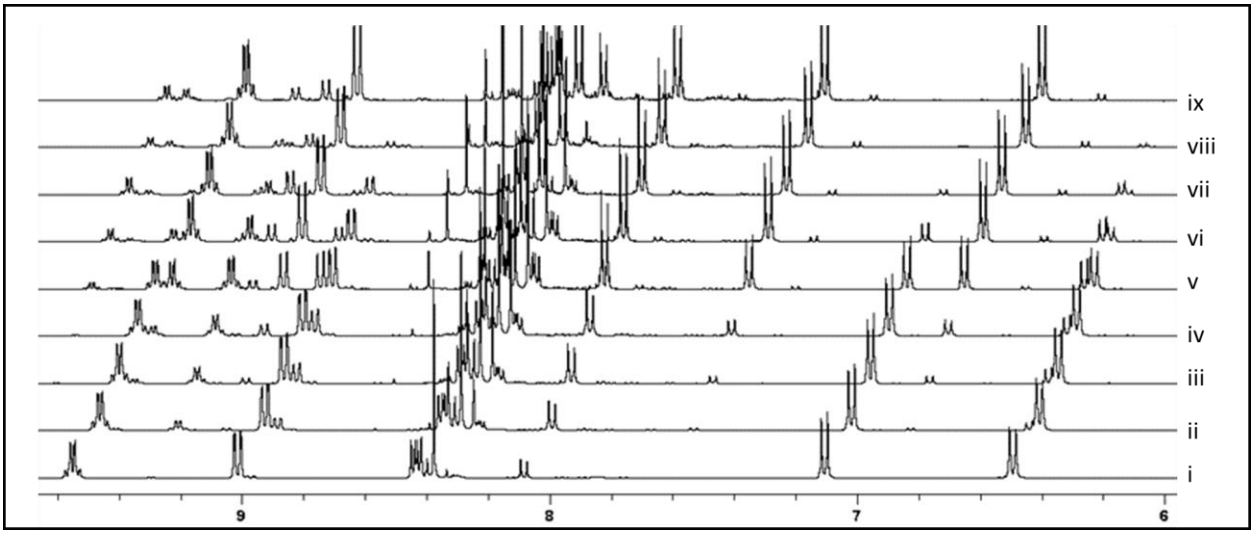

Figure 5: NMRs of 24 (CD3CN) over a period of exposure to air and light; i) initial product; ii) 30 minutes after exposure to air; iii) Irradiation for 1 hour; iv) Irradiation for 3 hours; v) Irradiation for 4 hours; vi) Irradiation for 6.5 hours; vii) Irradiation for 8.5 hours; viii) Irradiation for 9.5 hours; ix) Irradiation for 13.5 hours in total.

While in some cases (e.g. **21**) appreciable levels of dinuclear complex were only observed under photooxidation conditions, it should be noted that all these complexes appear to exist in equilibrium with the dinuclear complexes, with the equilibrium position dependent upon substituents. In addition to the observation above of dinuclear complexes in the DPPZ complex, **6**, NMR experiments in degassed solutions in amber tubes using Bphen/4-$MeOC_6H_4SH$, revealed that two major products, mononuclear and dinuclear, were present in 3:1 ratio, whereas the Bpy/PhSH pair gives only the mononuclear complex even under areobic conditions. Taken

together these findings suggest that the equilibrium position is ligand dependant with more electron rich thiols encouraging the formation of dinuclear complexes.

In summary, these platinum 1,2-diimine thiolate complexes appear to exist in equilibrium with thiol-bridged dinuclear complexes, with the equilibrium position being substituent dependent; under irradiation and in the presence of air, the equilibrium shift to favour dinuclear complexes as free thiol is converted to disulphides; the dinuclear complexes are then further S-oxidised to mononuclear sulphinate complexes and upon prolonged irradiation the sulphinates are oxidised to the sulphonic acids which dissociate, meanwhile the platinum complex reforms the starting iodide or an aqua complex.

Summary of Steps

Based on these results, and the previous demonstration that the photo-excitation of these complexes involves charge transfer from the coordinated sulphur to the N^N ligand, a series of likely steps can be proposed (Scheme 8):-

1. $N\hat{}N\text{-}PtMe_3\text{-}SR \leftrightharpoons [(N\hat{}N\text{-}PtMe_3)_2\text{-}SR]^+[RS]^-$

-mononuclear and dinuclear complex in equilibrium

2. $N\hat{}N\text{-}PtMe_3\text{-}SR + h\nu + O_2 \rightarrow$ (via $N\hat{}N^{\cdot-}\text{-}PtMe_3\text{-}S^{\cdot+}R$) $\rightarrow [N\hat{}N\text{-}PtMe_3\text{-}SR]^+ + O_2^-$

-photoexcitation to the excited state followed by SET to O_2 (as both $h\nu$ and O_2 are required) with concomitant reduction of dioxygen to superoxide (other ROS cannot be excluded)

3. $[(N\hat{}N\text{-}PtMe_3)_2\text{-}SR]^+[RS]^- + [N\hat{}N\text{-}PtMe_3\text{-}SR]^+ \rightarrow [(N\hat{}N\text{-}PtMe_3)_2\text{-}SR]^+ + N\hat{}N\text{-}PtMe_3\text{-}SR] + ½\ RSSR$

-oxidation of thiolate anion to disulphide by the radical cation derived from the photoexcited state of the mononuclear complex

4. $[(N\hat{}N\text{-}PtMe_3)_2\text{-}SR]^+ + O_2$ (via ROS) $\rightarrow N\hat{}N\text{-}PtMe_3\text{-}SO_2R + [N\hat{}N\text{-}PtMe_3]^+$

-oxidation of the bridging thiolate (stepwise or concerted) to the sulphinate complex with loss of the uncordinated Pt core – we have no data concerning intermediates but this step is only observed from the dinuclear complex.

5. $N^N\text{-}PtMe_3\text{-}SO_2R + ROS \rightarrow [N^N\text{-}PtMe_3]^+ + [RSO_3]^-$

-oxidation of the sulphinate to the sulphonic acid.

The combination of steps 2 and 3 indicate that the complex photocatalyses the oxidation of thiols to disulphides, which was supported by irradiating an NMR tube containg reduced glutathione and complex **22** in D_2O/d_3-MeCN which showed an irradiation-dependent oxidation to the disulphide form.

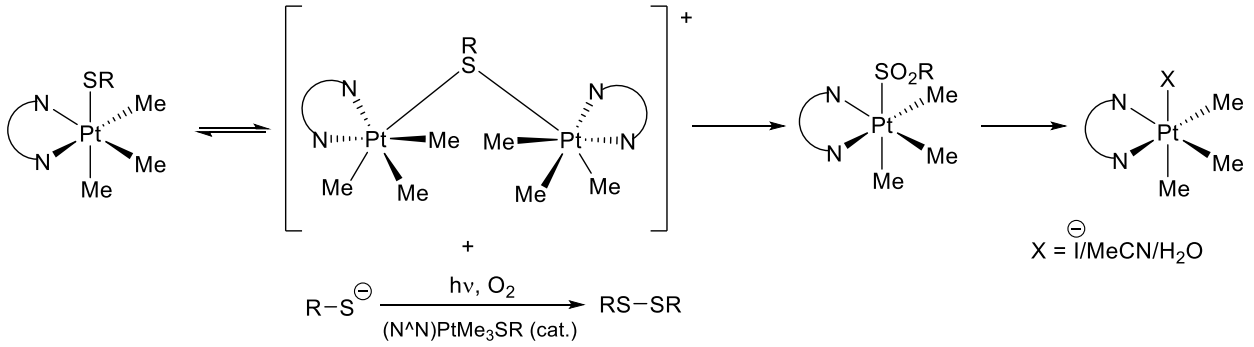

Scheme 8: Suggested pathway for the decomposition of [(N^N)PtMe3SR]

4-Nitrophenyl Sulphinate complexes 26-29.

The 4-nitrosulphinate complexes isolated from the reaction of 4-nitrothiophenol with complexes **1**-**4**, were more stable than complexes previously discussed in this report, allowing partial characterisation. Although these complexes are intrinsically unstable and degrade even in the solid state over several days, they were at least long lived enough to allow NMR and photophysical characterization on clean materials. NMR analysis confirmed the mononuclear nature of the complexes and IR spectra showed stretches tentatively assigned to S=O at higher wave number

(average ~1220 cm^{-1}) than the Ni(II) precedents (average ~1190 cm^{-1}), in line with the higher oxidation state in the Pt (IV) complexes reducing the back bonding and strengthening the S=O bonds. The reason for the higher stability of sulphinate complexes derived from 4-nitrothiophenol compared to other thiols is not entirely clear, but may be related to Pt-S=O back bonding. However, complex **30** in which back bonding to S=O should be maximised by the electron-donating 4,4'-dimethoxy-2,2'-bipyridine unit, was itself unstable and not able to be characterised beyond a crystal structure. The Pt-S bond lengths in the 4-nitrothiophenolate series (2.40-2.45 Å) are within the range of the two examples of sulphinate complexes previously discussed (2.39, 2.55 Å) which is compatible with, although not empirical evidence for, a back-bonding explanation. However, it should be noted that stability is a kinetic concept and bond length thermodynamic, and without much greater insight into the mechanism of loss of the sulphinate ligand speculation about the bearing of back bonding on the activation energy would be misguided.

Photophysical Characteristics of 4-Nitrophenyl Sulphinate complexes 26-29.

With a series of at least reasonably stable platinum(IV)trimethyl1,2-diimine thiophenolate complexes finally available in the form of the oxidised sulphinate series **26** - **29** their absorption and emission properties were studied in solution. Complexes **26** – **29** all display similar absorption spectra across a range of concentrations: they have a sharp, high energy peak between 273 – 286 nm (Figure 6) assigned to spin-allowed π - π^* ligand transitions of the 1,2-diimines mixed with spin allowed singlet MLCT (d-π^*) as previously reported for platinum trimethyl 1,2-diimines.[13,14] In addition there was a broad, lower energy peak of much lower intensity between 364 – 485 nm (Figure 7) observed in all the complexes and which is the absorption band related to the characteristic colours of the complexes. The nature of this absorption band is discussed below.

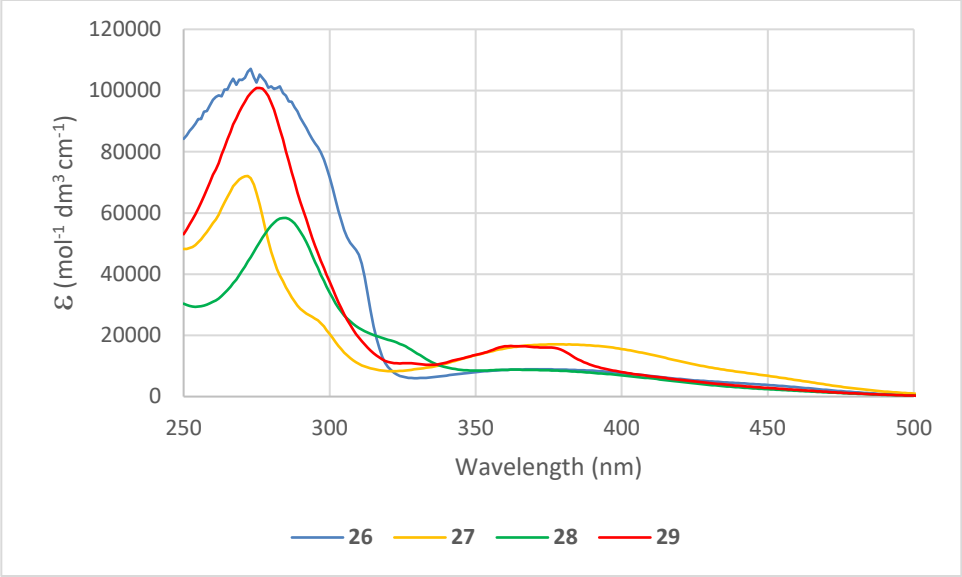

Figure 6. Absorption spectra of complexes **26** - **29** in MeCN

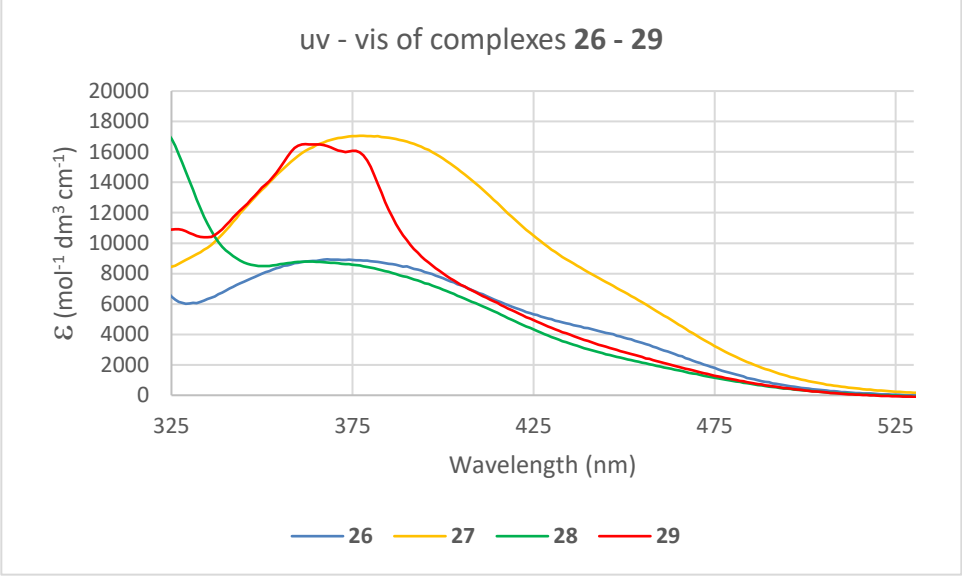

Figure 7. Expansion of absorption spectra of **26** - **29** between 325 and 530 nm

In addition to the electronic absorption spectra, excitation and emission spectra were recorded of complexes 26-29 and revealed broad emission bands with maxima between 410-500 nm and broad excitation bands with maxima between 280-340 nm (see table 3, Figure 8). They also show

very weak broad shoulders tailing to low energy (>550 nm) which are only significant in weakly emitting, over-concentrated samples where they can appear stronger. This distortion is due to inner filter and absorption effects whereby, in the case of these complexes, the higher energy end of the emission bands have significant overlap with the lower energy (non-emissive) absorption bands, biasing detection to the lower energy shoulders in concentrated samples. The luminescence quantum yields were determined to be between 0.02 – 0.1%, comparable to the previously reported values for $PtMe_3$(N^N)thiophenolates of 0.04%.[14] TCSPC gave data which fitted well to single exponential decays solving to give luminescence lifetimes in the 1 – 10 ns region. The low energy shoulders are apparently of the same electronic origin as the main bands as no second lifetime component could be detected shifting the detection wavelength (although these data were poor due to weak counts). These excitation and emission characteristics are closely related to other reports of emission from platinum (IV) trimethyl 1,2-diimine complexes[13,14] but are of interest as they appear to show that the low energy absorption detected in the uv vis absorption spectrum leads to a non-emissive state, and that only excitation at higher energy populated an emissive state. The excitation spectra do not match the absorption spectra, with excitation maxima matching the low energy shoulder of the strongest absorption peaks centred around 300 nm, and with the low energy absorption bands in the visible region not reflected at all in the excitation spectra. It is expected that the lower energy shoulder of the strongest absorption bands reflects transitions in the more conjugated N^N ligands with higher energy contributions from the less conjugated aryl sulphinate unit, implying that the emissive state is localised on the conjugated system. The lifetimes of 1-10 ns are short in comparison to triplet emitting transition metal complexes and as sensitivity to $^3O_2$ is a common probe for triplet states, lifetime measurements were recorded on degassed samples. There was very little change to the average lifetimes recorded (<1ns) indicating that quenching by

$^3O_2$ is not responsible for the fast decay of the excited states. As a comparison, the lifetime of Pt(Me_3)(bpy)-4-methoxycarbonylthiophenolate **22** which has previously been reported as a triplet emitter[14] was recorded and found to be 5.6 ns. Finally, Pt(Me_3)(bpy)I, again a known triplet emitter[12] was found to have a lifetime of 2.8 ns indicating that these short lifetimes are typical of this core. In the light of these comparisons, the magnitude of the quantum yields, and the large Stokes shifts, it seems most likely that these complexes emit from triplet states but are quenched by structural features (e.g. the nine C-H bonds close to the location of the excited state) rather than $^3O_2$.

Complex	1,2-Diimine	$\lambda_{max(abs)}$ (nm);ε(mol^{-1} dm^3 cm^{-1})	$\lambda_{max(ex)}$ (nm)	$\lambda_{max(em)}$ (nm)	Θ_F[a]	τ(ns)
26	2,2'-bipyridine	272(107094) 374(8612)	330	415	$8.9x10^{-4}$	1.24[b]
27	1,10-phenanthroline	274(71323) 380(17046)	336	407	$2.3x10^{-4}$	N/A[c]
28	4,7-diphenyl-1,10-phenanthroline	291(57822) 366(8763)	342	456	$9.7x10^{-4}$	10.3[d]
29	dipyrido[3,2-a:2',3'-c]phenazine	291(57822) 363(16499	335	425	$4.9x10^{-4}$	N/A[c]

Table 3. Excitation and emission data of complex **26** - **29** in MeCN a) Estimated relative to standard,[30] see SI for detail. b) Excited at 405 nm, χ^2=1.024. c) no excitation wavelength gave adequate counts. d) Excited at 375 nm, χ^2=1.104.

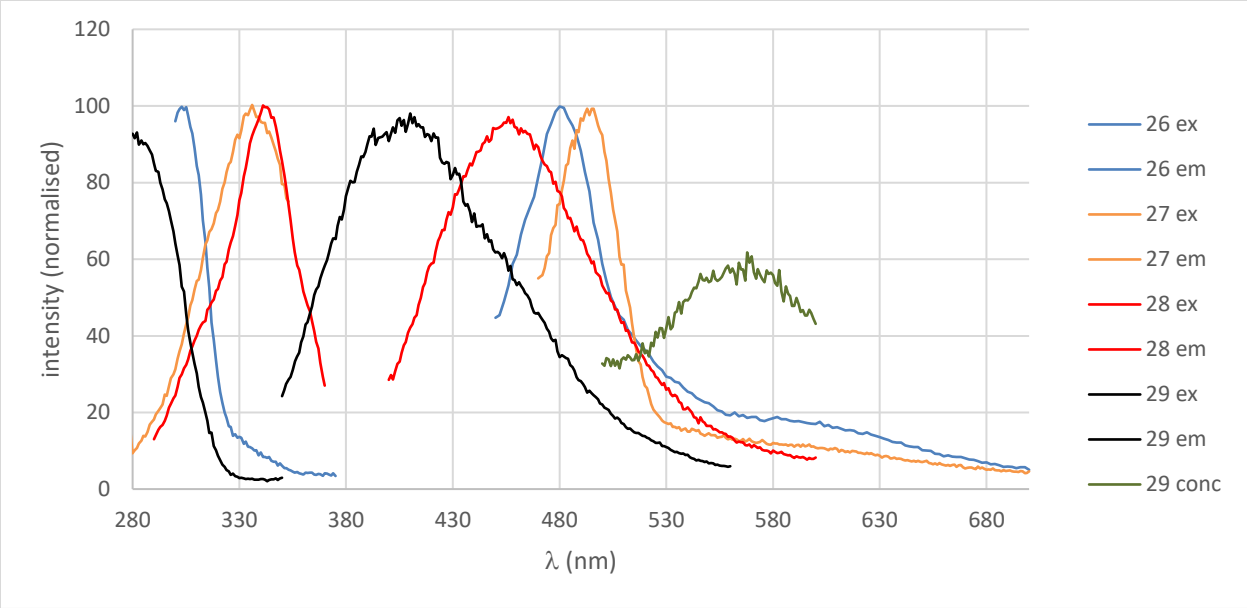

Figure 8 Excitation and emission spectra of complexes **26** - **29** in MeCN

The orbital origin of the low energy absorbances were unclear, as the low energy absorbance bands responsible for visible light excitation of platinum (IV) trimethyl 1,2-diimine thiolates have been assigned as originating from excitation of electrons in a mixed Pt-S σ bonding and sulphur lone pair non-bonding electrons.[14] As the sulphur in the sulphinate complexes has no non-bonding electrons it seemed unlikely that the Pt-S σ orbitals could be the sole donor and further clarification was sought through theoretical work.

Theoretical Studies of Sulphinate complexes

DFT calculations using the CAM-B3LYP level[31], with 6-31+G(d,p) basis set on light atoms and SDD on Pt[32] in simulated CH_3CN[33] indicated the HOMO of **26** to be a mixture of Pt-S and Pt-$C_{(Me\text{-}trans\ to\ S)}$ σ- bonding orbitals and the LUMO of π* character located on the 4-nitrothiophenolate ligand rather than the bipyridine (Figure 9). The LUMO +1 of **26** is also of π* character but based on the bipyridine ligand, and approximately 0.47 eV higher in energy than the LUMO. HOMO-LUMO absorption is predicted to lie at 319 nm (f = 0.058), while HOMO-LUMO+1 is predicted

to absorb at 292 nm (f = 0.021). The HOMO-1 orbital is of π character and based on the bipyridine ligand giving a HOMO-1 to LUMO+1 (i.e. π to π*) transition with strong absorption (f = 0.33) at 271 nm.

In the light of these findings we suggest that the lowest energy absorption observed in the spectra of **26 – 29** are assigned to a spin allowed singlet HOMO→LUMO σ (Pt-S/Pt-C) → π* (Ar-NO_2) transition, leading to a non-emissive excited state, while the higher energy excitations combine a HOMO→LUMO+1 σ (Pt-S/Pt-C) → π* (1,2-diimine) transition, and a much stronger HOMO-1 → LUMO+1 π to π* transition, which leads to the emissive state, analogous to those observed in related complexes.[12,14] It is unusual for a higher state not to relax into a lower one, but, given that relaxation into the Ar-NO_2-based state must be to the same spin multiplicity as the N^N state from which it originates, and given that the excitation to the Ar-NO_2-based singlet state is itself significantly lower energy than that to the N^N state, then assuming an Ar-NO_2-based triplet of even lower energy, intersystem crossing may be inefficient due to poor vibrational overlap of the states, in line with energy-gap law. For efficient relaxation between different sections of a luminophore without significant vibrational overlap there is a requirement for a dipole-dipole mechanism to allow relaxation of one state to populate the excited state of the other, and in the absence of this it is common to see phenomena such as dual emission. In the case of complex **26**, the TD-DFT transition dipoles corresponding to absorptions at 319 and 292 nm are almost perpendicular (θ = 106.6°), possibly indicating an inefficient dipole-dipole coupling and therefore inefficient relaxation.

While the explanation for the lack of relaxation through the non-emissive LUMO (sulphinate-based) excited state is speculative, a novel excitation mechanism involving a σ (Pt-S/Pt-C) → π* (Ar-NO_2) transition has been revealed by DFT methods. In addition to this unusual excited state,

the emissive 1,2-diimine-based state has also been shown to be of an unusual origin again involving a HOMO containing Pt-C σ bond character. To the best of our knowledge transitions of these natures have not been previously reported.

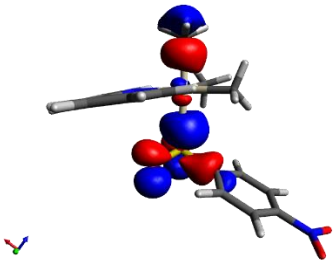

HOMO of **26**

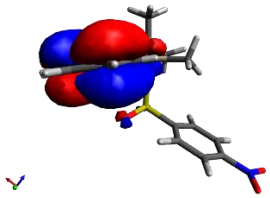

HOMO-1 of **26**

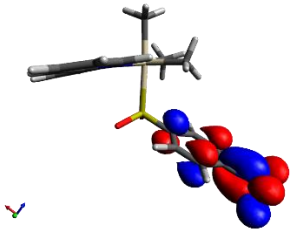

LUMO of **26**

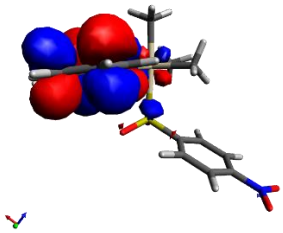

LUMO+1 of **26**

Figure 9 Molecular orbitals of complex **26**.

In order to verify that the new transition discovered for complex **26** was a feature of the nitro-substituted thiophenol unit, analogous calculations were performed for the (unknown) nitro-free sulphinate complex $PtMe_3(bpy)SO_2C_6H_5$, **30**. The HOMO was again a mixture of Pt-S and Pt-$C_{(Me\text{-}trans\ to\ S)}$ σ- bonding orbitals, but the LUMO in this case was the bipyridine π* orbital, giving a HOMO→LUMO allowed singlet transition of similar character and energy to the HOMO→LUMO+1 transition of **29** (Figure 10). The HOMO-1 of **30** is of π* character located on

both the bipyridine and the thiolate, giving a HOMO-1→LUMO transition of π→ π* nature. Thus while the low energy transition to the sulphinate π* is unique to the nitro substituted case, it appears that the HOMO of the sulphinate complexes are generally of Pt-S and Pt-$C_{(Me\text{-}trans\ to\ S)}$ σ- bonding character. The existence of this relatively high energy HOMO in all oxidised complexes is significant in light of the observation that even oxidised complexes continue to show photooxidation ability – i.e. the loss of the thiolate lone pair does not preclude photocatalytic ability.

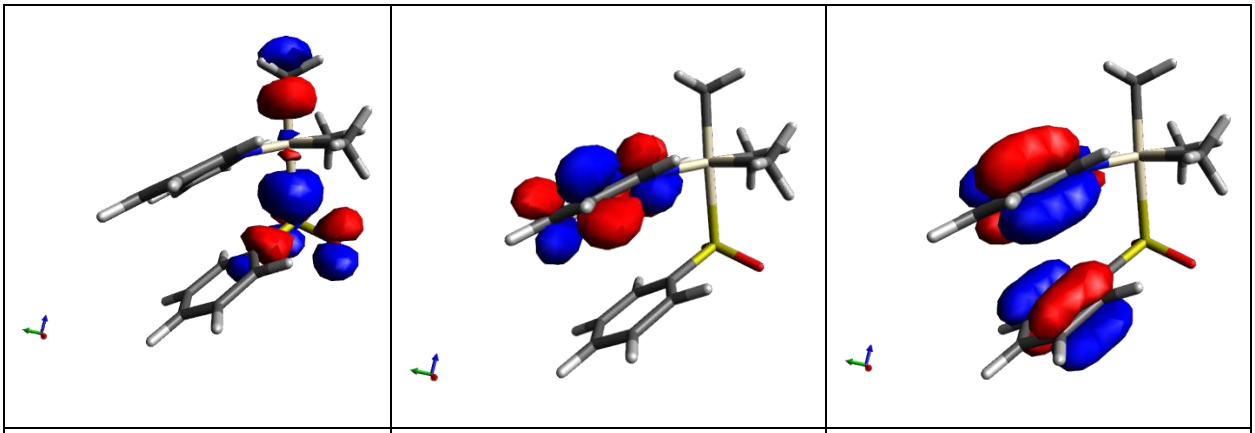

HOMO of **30**	LUMO of **30**	HOMO-1 of **30**

Figure 10. Molecular orbitals of **30**.

Conclusions

Although this study initially set out to explore the luminescent properties of platinum (IV) trimethyl bipyridyl thiolate complexes and their potential for luminescence applications it is now apparent that there is rich and complicated chemistry associated with these systems. These complexes appear to exist in dynamic equilibrium with dinuclear Pt (IV) S-bridged complexes, the position of the equilibrium being a function of the nature of both the 1,2-diimine and thiolate ligands. The complexes show photochemical reactivity with visible light excitation with initial oxidation of the thiolate counterion trapping them in the dinuclear form, then photooxidation to

the sulphinate complexes. There is precedent for dinuclear complex formation in $Pt(Me_3)$1,2-diimine based systems,[23] but there are no previous reports of Pt(IV) sulphinates. In a recent report the closely related $Re(CO)_3$1,2-diimine thiophenolates are described as undergoing degradation in solution to materials which have not been characterized but in which the NMR signals are similar to those observed in our photochemical oxidations.[34] Although a number of dinuclear and sulphinate complexes have been characterised by X-ray crystallography, and an outline mechanism for the transformation suggested by NMR studies, the sulphinate complexes are generally unstable and the sulphinate is displaced by solvent, water or halides. However, sulphinates derived from 4-nitrothiophenol give complexes which are sufficiently stable to allow some degree of characterisation to be undertaken. This stability can be rationalised in terms of back-bonding into the sulphinate π* by the d^6 Pt(IV) core. The sulphinate complexes show unusual photophysical behaviour with excitations from a HOMO which is based in a mixed σ (Pt-S/Pt-C) bonding orbital to LUMOs of π* symmetry based on either the N^N ligand, or, in the case of nitro-substituted species, the sulphinate aromatic ring. The transition to the sulphinate ring leads to a non-emissive state, while excitation to the N^N derived π* orbitals gives emission with large Stokes shifts and these states do not interconvert.

Supporting Information.

The following files are available free of charge. SI which contains: Descriptions of experimental procedures and spectral data for the meta-stable complexes mentioned in the text; details of the analysis of NMR experiments pertinent to mechanistic work; decay and fitting data used to calculate the luminescence lifetimes; crystallographic data for all structures reported in the manuscript.

Conflict of Interest Disclosure

The authors declare no competing financial interest.

Corresponding Author

*Michael P. Coogan, m.coogan@lancaster.ac.uk

Author Contributions

The manuscript was written through contributions of all authors. All authors have given approval to the final version of the manuscript. ‡These authors contributed equally.

Funding Sources

Royal Society of Chemistry Undergraduate Research Bursary (to CMAF)

ACKNOWLEDGMENTS

We thank Dr David Rochester, Department of Chemistry, Lancaster University, for mass spectrometry and the Royal Society of Chemistry for a Royal Society of Chemistry Undergraduate Research Bursary (to CMAF).

REFERENCES

(1) D. Ravelli, D. Dondi, M. Fagnoni and A. Albini, Photocatalysis. A multi-faceted concept for green chemistry *Chem. Soc. Rev*., **2009**, *38*, 1999-2011.

(2) Y. Chi and P.-T. Chou, Transition-metal phosphors with cyclometalating ligands: fundamentals and applications *Chem. Soc. Rev*., **2010**, *39*, 638-655.

(3) D. G. Nocera, Living healthy on a dying planet *Chem. Soc. Rev*., **2009**, *38*, 13-15.

(4) Vanesa Fernández-Moreira, Flora L. Thorp-Greenwood and Michael P. Coogan Application of d6 transition metal complexes in fluorescence cell imaging. *Chem. Commun*., **2010**, *46*, 186-202

(5) E. Turner, N. Bakken and J. Li, Cyclometalated platinum complexes with luminescent quantum yields approaching 100%, *Inorg. Chem*., **2013**, *52*(13), 7344-7351.

(6) S. W. Botchway, M. Charnley, J. W. Haycock, A. W. Parker, D. L. Rochester, J. A. Weinstein and J. A. G. Williams, Time-resolved and two-photon emission imaging microscopy of live cells with inert platinum complexes, *Proc. Natl. Acad. Sci. U. S. A*., **2008**, *105*(42), 16071-16076. C.-K. Koo, K. Wong, C. W.-Y. Man, Y.-W. Lam, L. K.-Y. So, H.-L. Tam, S.-W. Tsao, K.-W. Cheah, K.-C. Lau, Y.-Y. Yang, J.-C. Chen and M. H.-W. Lam, A Bioaccumulative Cyclometalated Platinum(II) Complex with Two-Photon-Induced Emission for Live Cell Imaging, *Inorg. Chem*., **2009**, *48*(3), 872-878.

(7) F. Juliá, D. Bautista and P. González-Herrero, Developing strongly luminescent platinum(iv) complexes: facile synthesis of bis-cyclometalated neutral emitters, *Chem. Commun.*, **2016**, *2*(8), 1657–1660.

(8) L. Chassot, A. von Zelewsky, D. Sandrini, M. Maestri and V. Balzani, Photochemical preparation of luminescent platinum(IV) complexes via oxidative addition on luminescent platinum(II) complexes, *J. Am. Chem. Soc.*, **1986**, *108(19)*, 6084–6085.

(9) A. Abedi, V. Amani, N. Safari, S. N. Ostad and B. Notash, From proton transferred to cyclometalated platinum(IV) complex: Crystal structure and biological activity, *J. Organomet. Chem.*, **2015**, *799–800*, 30–37.

(10) F. Juliá, D. Bautista, J. M. Fernández-Hernández and P. González-Herrero, Homoleptic tris-cyclometalated platinum(iv) complexes: a new class of long-lived, highly efficient 3LC emitters, *Chem. Sci.*, **2014**, *5*, 1875.

(11) W. J. Pope and S. J. Peachey, A new class of organo-metallic compounds. Preliminary notice. Trimethylplatinimethyl hydroxide and its salts. *Proc. Chem. Soc*, **1907**, *23*, 86.

(12) H. Kunkely and A. Vogler, Electronic spectra and photochemistry of methyl platinum(IV) complexes, *Coord. Chem. Rev.*, **1991**, *111*, 15–25; J. E. Hux and R. J. Puddephatt, Photochemistry of mononuclear and binuclear tetramethylplatinum(IV) complexes: Reactivity of an organometallic free radical, *J. Organomet. Chem*., **1992**, *437*(1-2), 251-263. J. E. Hux and R. J. Puddephatt, Photochemistry of tetramethyl(2,2'-bipyridine)platinum(IV), *J. Organomet. Chem*., **1988,** *346*(1), C31-C34; Fiona S. Mackay, Nicola J. Farrer, Luca Salassa, Hui-Chung Tai, Robert J. Deeth, Stephen A. Moggach, Peter A. Wood, Simon Parsons and Peter J. Sadler, Synthesis, characterisation and photochemistry of Pt(IV) pyridyl azido acetato complexes, *Dalton Trans*., **2009**, 2315-2325.

(13) J. E. Hux and R. J. Puddephatt, Reactivity of tetramethylplatinum(IV) complexes: Thermal reactions with electrophiles and unsaturated reagents, *Inorg. Chim. Acta*, **1985**, 100(1), 1-5; M. S. McCready and R. J. Puddephatt, Oxidative addition of functional disulfides to platinum(II): Formation of chelating and bridging thiolate–carboxylate complexes of platinum(IV), *Inorg. Chem. Commun.*, **2011**, *14*, 210–212. Vetter, Cornelia; Wagner, Christoph; Schmidt, Juergen; Steinborn, Dirk, Synthesis and characterization of platinum(IV) complexes with N,S and S,S heterocyclic ligands, *Inorg. Chim. Acta*, **2006**, *359*(13), 4326-4334. Brown, B. W.; Kite, K.; Nettle, A. J.; Psaila, A. F., Complexes of trimethylplatinum(IV) with dithiocarbamates, xanthates and cis-

maleonitriledithiolate *J. Organomet. Chem*., **1977**, *139*(1), C1-C3. Hall, J. R.; Swile, G. A. Proton NMR and infrared spectra of trimethylplatinum(IV) complexes of β-diketones, thio-β-diketones, and β-iminoketones, *J. Organomet. Chem*., **1973**, *47*(1), 195-215.

(14) H. L. Steel, S. L. Allinson, J. Andre, M. P. Coogan and J. A. Platts, Platinum trimethyl bipyridyl thiolates - New, tunable, red- to near IR emitting luminophores for bioimaging applications, *Chem. Commun.*, **2015**, *51(57),* 11441–11444.

(15) Javier Troyano, Oscar Castillo, Jose I. Martinez, Vanesa Fernandez-Moreira, Yolanda Ballesteros, Daniel Maspoch, Felix Zamora and Salome Delgado, Reversible Thermochromic Polymeric Thin Films Made of Ultrathin 2D Crystals of Coordination Polymers Based on Copper(I)-Thiophenolates, *Adv. Funct. Mater*. **2018**, *28*(5) 1704040.

(16) Gaussian 09, Revision D.01, M. J. Frisch, G. W. Trucks, H. B. Schlegel, G. E. Scuseria, M. A. Robb, J. R. Cheeseman, G. Scalmani, V. Barone, B. Mennucci, G. A. Petersson, H. Nakatsuji, M. Caricato, X. Li, H. P. Hratchian, A. F. Izmaylov, J. Bloino, G. Zheng, J. L. Sonnenberg, M. Hada, M. Ehara, K. Toyota, R. Fukuda, J. Hasegawa, M. Ishida, T. Nakajima, Y. Honda, O. Kitao, H. Nakai, T. Vreven, J. A. Montgomery, Jr., J. E. Peralta, F. Ogliaro, M. Bearpark, J. J. Heyd, E. Brothers, K. N. Kudin, V. N. Staroverov, T. Keith, R. Kobayashi, J. Normand, K. Raghavachari, A. Rendell, J. C. Burant, S. S. Iyengar, J. Tomasi, M. Cossi, N. Rega, J. M. Millam, M. Klene, J. E. Knox, J. B. Cross, V. Bakken, C. Adamo, J. Jaramillo, R. Gomperts, R. E. Stratmann, O. Yazyev, A. J. Austin, R. Cammi, C. Pomelli, J. W. Ochterski, R. L. Martin, K. Morokuma, V. G. Zakrzewski, G. A. Voth, P. Salvador, J. J. Dannenberg, S. Dapprich, A. D. Daniels, O. Farkas, J. B. Foresman, J. V. Ortiz, J. Cioslowski, and D. J. Fox, Gaussian, Inc., Wallingford CT, 2013.

(17) a. Y. Zhao and D. G. Truhlar, "The M06 suite of density functionals for main group thermochemistry, thermochemical kinetics, noncovalent interactions, excited states, and transition elements: two new functionals and systematic testing of four M06-class functionals and 12 other functionals," *Theor. Chem. Acc*., **2008,** *120*, 215-41. b. R. Ditchfield, W. J. Hehre, and J. A. Pople, "Self-Consistent Molecular Orbital Methods. 9. Extended Gaussian-type basis for molecular-orbital studies of organic molecules," *J. Chem. Phys*., **1971,** *54*, 724. c. P. C. Hariharan and J. A. Pople, "Influence of polarization functions on molecular-orbital hydrogenation energies," *Theor. Chem. Acc.*, **1973,** *28*, 213-22. d. D. Andrae, U. Haeussermann, M. Dolg, H. Stoll, and H. Preuss, "Energy-adjusted ab initio pseudopotentials for the 2nd and 3rd row transition-elements," *Theor. Chem. Acc.*, **1990,** *77*, 123-41.

(18) T. Yanai, D. Tew, and N. Handy, "A new hybrid exchange-correlation functional using the Coulomb-attenuating method (CAM-B3LYP)," *Chem. Phys. Lett*., **2004,** *393*, 51-57.

(19) J. Tomasi, B. Mennucci, and R. Cammi, "Quantum mechanical continuum solvation models," *Chem. Rev*., **2005**, 105, 2999-3093.

(20) O. V. Dolomanov, L. J. Bourhis, R. J. Gildea, J. A. K. Howard and H. Puschmann, OLEX2: a complete structure solution, refinement and analysis program, *J. Appl. Cryst*., **2009,** *42*, 339-341.

(21) G. M. Sheldrick, Crystal structure refinement with SHELXL, *Acta Cryst*., **2015,** *C71*, 3-8.

(22) L. J. Farrugia, WinGX and ORTEP for Windows: an update, J. Appl. Cryst., **2012**, *45*, 849-854.

(23) G. S. Hill, J. J. Vittal, and R. J. Puddephatt, Methyl(hydrido)platinum(IV) Complexes: X-ray Structure of the First (μ-Hydrido)diplatinum(IV) Complex, *Organometallics* **1997**, 16(6),

1209–1217; B.Vance, Crystal structure of tetrakis(trimethyl-μ-S,S,N-thiocyanatoplatinum), [{Pt(CH3)$_3$SCN}$_4$] *J. Organomet. Chem*., **1987**, *336*(3), 441; K.H.Ebert, W.Massa, H.Donath, J.Lorberth, B.-S.Seo, E.Herdtweck, Organoplatinum compounds: VI1. Trimethylplatinum thiomethylate and trimethylplatinum iodide. The crystal structures of [(CH$_3$)$_3$PtS(CH$_3$)]$_4$ and [(CH$_3$)$_3$PtI]$_4$·0.5CH$_3$I, *J. Organomet. Chem*., **1998**, *559(1-2)*, 203; W.Clegg, N.Duran, K.A.Fraser, P.Gonzalez-Duarte, J.Sola, I.C.Taylor, New confacial bioctahedral diplatinum(IV) complexes with 3-aminoalkanethiolate bridges, *Dalton Transactions*, **1993**, *23*, 3453; D.C.Craig, I.G.Dance, Molecular structure of tetrakis[benzenethiolatotrimethylplatinum(IV)], (μ3-SPh)$_4$(PtMe$_3$)$_4$ *Polyhedron*, **1987**, *6(5)*, 1157; G.Smith, C.H.L.Kennard, T.C.W.Mak, The crystal structure of tetrakis[trimethylthiomethyl-platinum(IV)], [Pt(CH$_3$)$_3$(SCH$_3$)$_4$, *J. Organomet. Chem*., **1985**, *290(1)*, C7.

(24) *a)* M. S. Morton, R. J. Lachicotte, D. A. Vicic and W. D. Jones, Insertion of Elemental Sulfur and SO_2 into the Metal−Hydride and Metal−Carbon Bonds of Platinum Compounds *Organometallics*, **1999**, *18(2)*, 227–234; *b)* Y. Hu, A.Wojcicki, M.Calligaris, G.Nardin, Reactions of coordinatively unsaturated platinum(II)-.eta.1-allyl complexes with the electrophilic reagents sulfur dioxide, chlorosulfonyl isocyanate, and hexafluorophosphoric acid etherate, *Organometallics*, **1987**, *6(7)*, 1561; *c)* J.J.Stace, P.J.Ball, Vikas Shingade, S.Chatterjee, A.Shiveley, W.L.Fleeman, A.J.Staniszewski, J.A.Krause, W.B.Connick, Kinetics of the methylation of a platinum(II) diimine dithiolate complex, *Inorg. Chim. Acta*, **2016**, 447, 98; *d)* A.Ishii, S.Kashiura, Y.Hayashi, W.Weigand; Rearrangement of a (Dithiolato)platinum(II) Complex Formed by Reaction of Cyclic Disulfide 7,8-Dithiabicyclo[4.2.1]nona-2,4-diene with a Platinum(0) Complex: Oxidation of the Rearranged (Dithiolato)platinum(II) Complex, *Chem.-Eur. J.*, **2007**, *13(15)*, 4326; *e)* W. B. Connick, H. B. Gray, Photooxidation of Platinum(II) Diimine

Dithiolates, *J. Am. Chem. Soc.* **1997**, *119(48),* 11620; *f)* J. S.Hallock, A. S.Galiano-Roth, D. B. Collum; Organometallic chemistry of sulfinic acids. Highly stereo- and regioselective intramolecular hydroplatinations. X-ray crystal structure of $(Ph_3P)_2Pt[trans\text{-}SO_2CH(CH_3)CH_2CH(CH_2CH_3)]$, *Organometallics*, **1988**, *7*(12), 2486; *g)* L.M.Diamond, F.R.Knight, D.B.Cordes, A.L.Fuller, A.M.Z.Slawin, J.D. Woollins; Platinum bisphosphine complexes of 1,8-naphthosultone, *Polyhedron*, **2014**, *81*, 356; *h)* A. Oviedo, A. Arevalo, M. Flores-Alamo, J. J. Garcia, Mechanistic Insights into the C–S Bond Breaking in Dibenzothiophene Sulfones, *Organometallics* **2012**, *31(10),* 4039; *i)* A. Ishii, M. Ohishi, N. Nakata, Preparation of 3,3-Di-tert-butylthiirane trans-1,2-Dioxide and Its Reaction with a Platinum(0) Complex To Give a (Disulfenato)platinum(II) Complex: Regioselectivity of the Oxidation of a Related (Sulfenato–thiolato)platinum(II) Complex, *Eur. J. Inorg. Chem.* **2007**, *33*, 5199

(25) S. M. Aucott, H. L. Milto, S. D. Robertson, A. M. Z. Slawin, G. D. Walker and J. D. Woollins, Platinum Complexes of Naphthalene-1,8-dichalcogen and Related Polyaromatic Hydrocarbon Ligands, *Chem. - Eur. J.*, **2004,** *10*(7), 1666–1676.

(26) S. M. Aucott, P. Kilian, S. D. Robertson, A. M. Z. Slawin and J. D. Woollins, Platinum Complexes of Dibenzo[1,2]Dithiin, Dibenzo[1,2]Dithiin Oxides and Related Polyaromatic Hydrocarbon Ligands, *Chem. - Eur. J.*, **2006**, *12(3),* 895–902.

(27) The Cambridge Crystallographic Data Centre (CCDC), http://webcsd.cds.rsc.org/substructure_search.php (accessed 4th February 2021)

(28) R. M. Buonomo, I. Font, M. J. Maguire, J. H. Reibenspies, T. Tuntulani and M. Y. Darensbourg, Study of Sulfinate and Sulfenate Complexes Derived from the Oxygenation of

Thiolate Sulfur in [1,5-Bis(2-mercapto-2-methylpropyl)-1,5-diazacyclooctanato(2-)]nickel(II), *J. Am. Chem. Soc.*, **1995**, *117(3)*, 963–973.

(29) S.M. Nabavizadeh, S. Habibzadeh, M .Rashidi, R.J. Puddephatt. Oxidative Addition of Ethyl Iodide to a Dimethylplatinum(II) Complex: Unusually Large Kinetic Isotope Effects and Their Transition-State Implications *Organometallics* **2010**, *29(23)*, 6359-6368. B.Z. Momeni, M. Rashidi, M.M. Jafari, B.O. Patrick, A.S. Abd-El-Aziz, Oxidative addition of some mono, di or tetra haloalkanes to organoplatinum(II) complexes *J. Organomet. Chem*. **2012**, *700*, 83-92.

(30) K. Suzuki, A. Kobayashi, S. Kaneko, K. Takehira, T. Yoshihara, H. Ishida, Y. Shiina, S. Oishic and S. Tobita, Reevaluation of absolute luminescence quantum yields of standard solutions using a spectrometer with an integrating sphere and a back-thinned CCD detector *Phys. Chem. Chem. Phys.*, **2009**, *11*, 9850–9860.

(31) T. Yanai, D. Tew, and N. Handy, A new hybrid exchange–correlation functional using the Coulomb-attenuating method (CAM-B3LYP) *Chem. Phys. Lett.*, 2004, *393*(1-3), 51-57

(32) R. Ditchfield, W. J. Hehre, and J. A. Pople, Self-Consistent Molecular-Orbital Methods. IX. An Extended Gaussian-Type Basis for Molecular-Orbital Studies of Organic Molecules, *J. Chem. Phys.*, **1971**, *54*, 724; P. C. Hariharan and J. A. Pople, The influence of polarization functions on molecular orbital hydrogenation energies, *Theor. Chem. Acc.*, **973,** *28*, 213-22; D. Andrae, U. Haeussermann, M. Dolg, H. Stoll, and H. Preuss Energy-adjusted ab initio pseudopotentials for the second and third row transition elements, *Theor. Chem. Acc.*, **1990**, *77*(2), 123-41.

(33) J. Tomasi, B. Mennucci, and R. Cammi, Quantum Mechanical Continuum Solvation Models, *Chem. Rev.*,**2005**, *105*(8), 2999-3093

(34) M. He, H. Y. Vincent Ching, C. Policar and H. C. Bertrand, Rhenium tricarbonyl complexes with arenethiolate axial ligands, *New J. Chem.*, **2018**, *42*(14), 11312-11323

SYNOPSIS

$PtMe_3$bipyridine thiolates form S-bridged dinuclear complexes and show photochemical S-oxidation to photoluminescent sulphinates (Pt-SO_2Ar). DFT indicates that in addition to $\pi \rightarrow \pi^*$ transitions some of the photoreactivity and photophysics results from unexpected Pt-C/Pt-S $\sigma \rightarrow \pi^*$ transitions.

For table of contents only: